Theoretical Study of Ag Interactions in Amorphous Silica RRAM Devices

K. Patel [1,2], J. Cottom [1], M. Bosman [2,3], A. J. Kenyon [4] and A. L. Shluger [1]
[1]Department of Physics and Astronomy, University College London, Gower Street, London, WC1E 6BT, UK.
[2]Institute of Materials Research and Engineering, A*STAR (Agency for Science, Technology and Research), 2 Fusionopolis Way, Singapore 138634, Singapore.
[3]Department of Materials Science and Engineering, National University of Singapore, Singapore 117575, Singapore
[4]Department of Electrical & Electronic Engineering, University College London, Torrington Place, London, WC1E 7JE, UK.

In this study, Density Functional Theory (DFT) calculations were used to model the incorporation and diffusion of Ag in Ag/a-SiO_2/Pt resistive random-access memory (RRAM) devices. The Ag clustering mechanism is vital for understanding device operation and at this stage is unknown. In this paper an O vacancy (V_O) mediated cluster model is presented, where the V_O is identified as the principle site for Ag^+ reduction. The Ag^+ interstitial is energetically favored at the Fermi energies of Ag and Pt, indicating that Ag^+ ions are not reduced at the Pt electrode *via* electron tunneling. Instead, Ag^+ ions bind to V_O forming the $[Ag/V_O]^+$ complex, reducing Ag^+ *via* charge transfer from the Si atoms in the vacancy. The $[Ag/V_O]^+$ complex is then able to trap an electron forming $[Ag/V_O]^0$ at the Fermi energy of Pt. This complex is then able to act as a nucleation site for of Ag clustering with the formation of $[Ag_2/V_O]^+$ which is reduced by the above mechanism.

I. Introduction

In recent years, considerable effort has been devoted to the development of RRAM devices. High switching speeds, endurance and scalability combined with low power consumption make RRAM a viable alternative to FLASH memory [1]. RRAM devices operate *via* the resistive switching phenomenon, where the generation and dissolution of electron transport modes across a dielectric layer determine its resistance between high and low states. Typically, before this switching is observed, a conductive filament is formed across the dielectric layer in a process analogous to soft dielectric breakdown.

The nature of the conductive path varies with material and microstructure. Devices containing an oxide layer, typically amorphous SiO_2 (a-SiO_2), have been shown to operate under two distinct mechanisms; the electrochemical metallization mechanism (ECM) and the valence change mechanism (VCM) [2], [3]. As such, understanding how these mechanisms interact is important to the operation and optimization of RRAM devices. It is generally understood for ECM memories that metal ions migrate through the dielectric layer to the inert electrode *via* field-assisted diffusion. Metallic clusters then form, creating a conducting path across the dielectric. The specific oxidation and reduction processes remain unclear and are the subject of vigorous debate. An atomistic understanding of these processes is vital before the nucleation and propagation of metal clusters can be understood and optimized.

Ag/a-SiO_2/Pt devices have been studied extensively experimentally thus providing a wealth of experimental data for comparison with theoretical calculations [3]. The Ag_i and V_O-mediated mechanisms for Ag reduction and cluster nucleation are investigated in this work.

II. Methodology

The a-SiO_2 models were generated *via* molecular dynamics melt-quench using the ReaxFF [4] force field as implemented in the LAMMPS code [5]. The initial structure was a 216 atom supercell of cubic β-cristobalite (SiO_2). To ensure sufficient sampling of the amorphous structures was achieved, 30 models were generated. In each case the system was first equilibrated at 300 K and a pressure of 1 atm. The pressure was fixed at 1 atm whilst the temperature was linearly ramped to 5000 K using a Berendsen thermostat [6]. The temperature was maintained at 5000K for 40 ps to ensure the initial structure had been completely melted then cooled to 0 K at a rate of 8 K ps^{-1}. The final structures were then optimized using DFT with the PBE0-TC_LRC functional [7] in the CP2K code [8]. The densities (mean 2.20 g/cm^3), distributions of Si–O bonds and Si–O–Si angles, and neutron structure factors of the models were consistent with those obtained in previous studies [9], [10].

DFT calculations were carried out using the Gaussian Plane Wave method (GPW) [11] in the CP2K code. A plane wave cut-off and relative cut-off of 600 Ry and 40 Ry were used respectively, with double zeta valence polarized (DZVP) molecularly optimized (MOLOPT) basis sets [12] and Goedecker-Teter-Hutter (GTH) pseudopotentials [13]. The PBE0-TC-LRC functional truncated at 2 Å was used with the auxiliary density matrix method (ADMM) implementation to reduce computational cost [14].

To study the Ag interstitial and its charge states in a-SiO_2, the complete sampling of one supercell was carried out for the charge states $-1 \leq q \leq +2$. Out of the 30 produced models, the supercell with the density closest to the mean density was selected. A 3-dimensional grid with a 2 Å spacing was generated across the supercell giving 512 grid points. From these, grid points were excluded if there was a silica atom less than 1.34 Å away, corresponding to the atomic radius of Ag [15]. The remaining 259 points were used as initial Ag interstitial site locations. In separate simulations, Ag was added at each point and the geometry was optimized using the PBE functional. Unique sites were determined as those having any atom in the cell displaced by more than 0.2 Å, an energy difference of greater than 0.1 eV or a Mulliken charge difference of greater than 0.05 $|e|$. The unique sites were then optimized using the PBE0-TC-LRC functional.

The O vacancy was modelled at 37 sites in a periodic cell chosen using a ring sampling method, where each O in an N-membered ring was removed, and the geometry optimized ($N = 3 \leq N \leq 9$).

The defect formation energy, E_{form}, is calculated using the standard formalism of Northrup and Zhang [16]:

$$E_{form} = E_{defect} - E_{pristine} - \mu_x + q(\Delta E_F + E_v) + E_{corr},$$

where E_{defect} is the total energy of the system with the defect, $E_{pristine}$ is the total energy of the pristine system, μ_x is the chemical potential of chemical species, q is the charge of the system, ΔE_F is the Fermi level position, E_v is the potential alignment and E_{corr} is the charge correction. The Lany–Zunger finite size charge correction scheme was utilized to correct the formation energies of the charges defects [17]. The chemical potential of O, μ_O, is calculated as one half the energy of an O_2 molecule. The chemical potential of Ag, μ_{Ag}, is calculated from a 162-atom cell of Ag_2O as:

$$\mu_{Ag} = \frac{1}{2n}\left(E_{Ag_2O} - \frac{1}{2}n\mu_{O_2}\right),$$

where n is the number of Ag_2O units, E_{Ag2O} is the total energy of the Ag_2O system and μ_{O2} is the chemical potential of an O molecule. The Fermi energy positions of Ag and Pt have been experimentally measured at 4.96 eV and 4.11 eV with respect to the a-SiO_2 valence band respectively [18]–[20].

III. Results and Discussion

To understand the redox processes involved in Ag migration and clustering, it is first important to find the incorporation energy of Ag as a function of Fermi energy. From this, the charge state of Ag can be determined at the Ag and Pt electrodes under bias. Furthermore, studying the unique sites for Ag can gleam information about the accessible areas in a-SiO_2 during migration.

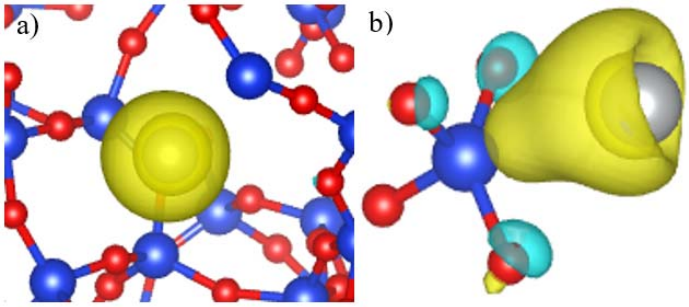

Fig. 1 Schematic showing the HOMO state of two configurations of the Ag^0 interstitial in a-SiO_2. The silver, blue and red spheres correspond to Ag, Si and O atoms respectively. The positive and negative charge density is shown as blue and yellow iso-surfaces respectively at a value of ± 0.07. a) Ag^0 occupies a void in the lattice, with the HOMO state mostly Ag s in character. b) Ag^0 resides near a wide O-Si-O angle bond, with charge donation from Ag to Si

In 18 out of the 34 unique sites found (Fig. 1a) Ag^0 is located in a void, where the highest occupied molecular orbital (HOMO) is primarily Ag s-character. In this case the mean Mulliken charge of Ag is 0.02 $|e|$. The remaining 16 sites (Fig. 1b) involve the widening of a proximate O-Si-O bond angle and the donation of charge from Ag to Si. Mulliken charge analysis gives a mean Ag charge of 0.25 $|e|$ and with a mean charge of 0.19 $|e|$ donated to the Si. Previous studies have shown that O-Si-O bond angles ≥ 130° are precursor sites for electron trapping [21]. Precursor sites can trap two electrons causing the weakening and stretching of an O-Si bond by 0.5 Å. This in turn results in lower barriers (~1 eV) for V_O formation [22]. In this study 13 of the 34 unique sites resulted in the sponaneous widening of an O-Si-O bond angle ≥ 130°.

The mean, minimum, and maximum incorporation energies of Ag^0 are 3.1 eV, 2.8 eV, and 6.1 eV respectively. The incorpoation energy of Ag^0 was found to be strongly correlated to the local steric environment. The coordination number (defined as the number of atoms within 3 Å of Ag^0) increases with the incorporation energy whilst the Mulliken charge on the Ag decreases. The Ag^0 atoms interacting with a widened O-Si-O bond angles have lower incorporation energies (~0.4 eV) than the void type defects with the same coordination number, suggesting the energetic cost of creating the wide angle O-Si-O is compensated by its interaction with Ag.

Analysis of the 50 unique Ag^+ ion sites shows that Ag^+ maintains a nearest neighbour distance of between 2.2 and 2.6 Å to an O in the lattice. This differs from Ag^0 where 18% of sites are in voids greater than 3 Å from their nearest neighbour. The mean Mulliken charge of Ag in the +1 state is 0.78 $|e|$, with a strong correlation to the crowding of the lattice around the ion. As with Ag^0, an increased coordination number yields a higher incorporation energy and a lower Mulliken charge (min/max ~ 0.4 $|e|$).

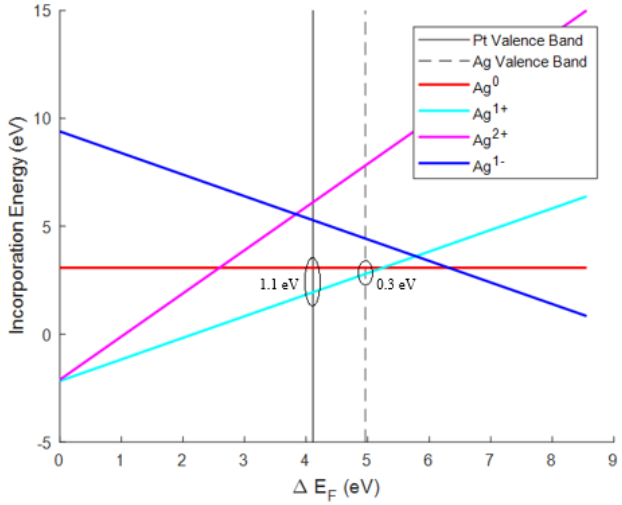

Fig. 2 Formation energy diagram of 259 Ag interstitial sites in a-SiO2

Fig. 2 shows the defect formation energy of Ag in a-SiO_2. The Fermi position of Ag relative to a-SiO_2 suggests that the mean defect formation energy of Ag^+ is 0.3 eV lower than Ag^0 at the Ag electrode under equilibrium with the mean (+1/0) transition at 5.25 eV. This is problematic in understanding RRAM operation as devices operate under bias with forming voltages as high as +10 V and switching voltages < +5 V. Under these conditions, the Fermi energy position of Ag would shift towards the silica conduction band. In this case, Ag^0 would be favored over Ag^+ meaning an alternative interaction must be involved in the Ag^+ ion generation process, with previous experiments suggesting the presence of water in devices playing a crucial role in ion generation [23], [24]. The switching mechanism in ECM memories is usually bi-polar with negative bias applied to reset the device. In this case, further calculations are required to study the

stability and charge transition levels of larger Ag clusters under operation.

Furthermore, from Fig. 2 we see that the defect formation energy of Ag^+ is 1.1 eV lower than that of Ag^0 at the Pt Fermi energy. This suggests that the reduction of Ag^+ ions by the tunneling of electrons from the Pt electrode is not energetically favorable. In this situation, Ag^+ ions are not reduced and clustering will not occur due to electrostatic repulsion between the charges. As such, the interaction of Ag with other defects in these devices is vital for understanding the redox processes. A plausible starting point is the V_O as the high bias applied across the dielectric may assist in V_O generation as seen in VCM devices.

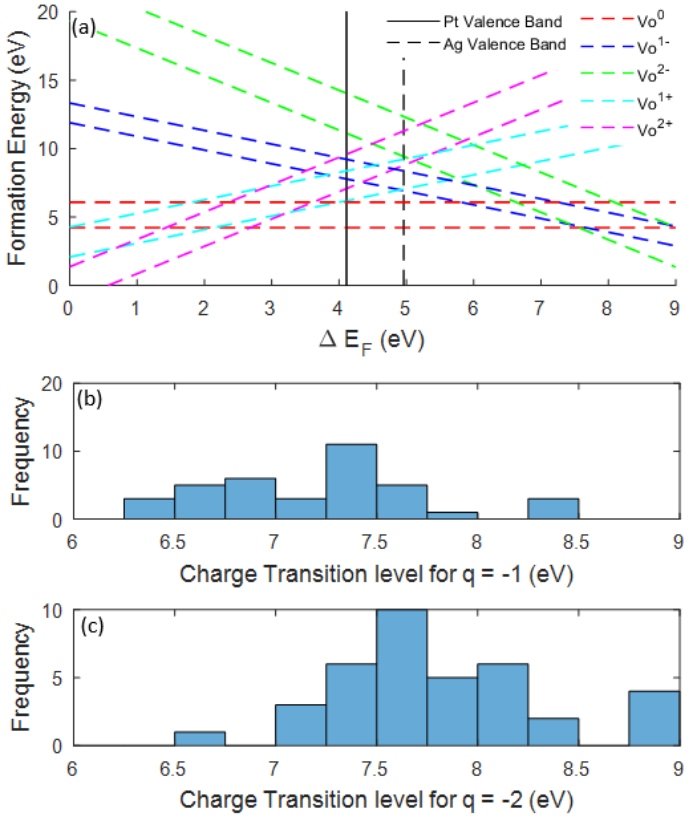

Fig. 3 a) Formation energies of 37 O vacancies as a function of Fermi energy, ΔEF, where ΔF = 0 at the VBM. The dashed lines represent maxima and minima in the data distribution. b) a histogram showing the (0/-1) charge transition position c) a histogram showing the (-1/-2) charge transition position.

Analysis of the 37 O vacancies give mean, minimum and maximum V_O formation energies of 5.3 eV, 4.2 eV and 6.1 eV; single and double electron trapping become favorable at $E_F > 7.2$ eV and 7.8 eV respectively suggesting that electron trapping may happen at 3 V. The calculations show a negative correlation of the (0/-1) and (-1/-2) transitions to the Si-Si bond length, suggesting that vacancies with short Si-Si bond lengths are energetically unfavorable to trap electrons. Fig. 4 compares the sampling method used in this study to the complete sampling of an a-SiO_2 cell, showing the data in this study is skewed due to the higher number of 2.3 Å to 2.4 Å bond lengths sampled. Correcting for this would yield a lower mean defect formation energy and also reduce the Fermi energy of the (0/-1) and (-1/-2) transitions.

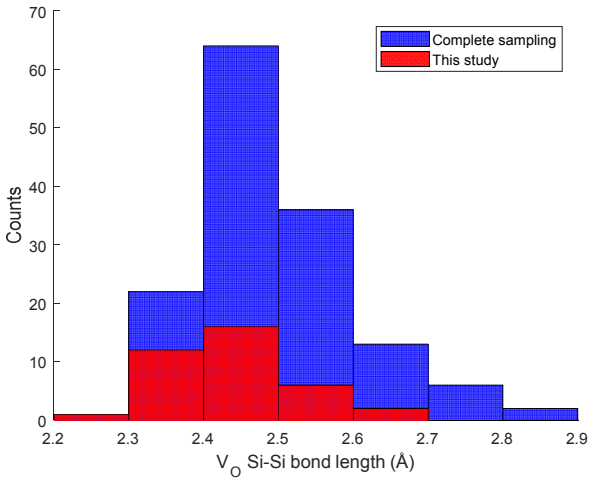

Fig 4. Histogram showing the Si-Si bond lengths for the V_O sampling method used in this study compared to a complete sampling method, where every O is removed from the cell [25].

As the neutral vacancy (V_O^0) is favored at the Fermi energy of both Ag and Pt, its interaction with Ag^+ is studied. For each of the 37 vacancies sampled, a Ag^+ ion was placed in between the contributing Si atoms and the geometry was relaxed. In 27 of the 37 sampled sites the ion interacts with the vacancy to form a $[Ag/Vo]^+$ complex. The mean Mulliken charge for Ag in the $[Ag/Vo]^+$ defect (Fig. 5a) is 0.17 $|e|$ compared to 0.82 $|e|$ for an Ag^{+1} interstitial. In this case, charge is donated from the Si atoms involved in the vacancy to Ag, showing the V_O to be a reduction site for Ag^+ ions. Ag can be further reduced by nearby oxygens to give a Mulliken charge of 0.05 $|e|$ (Fig. 5b) again highlighting the importance of local geometry on the Ag charge state.

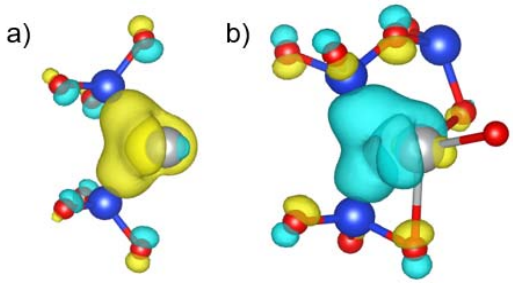

Fig. 5 Schematic showing the HOMO state of two configurations of the $[Ag/V_o]^+$ defect. The silver, blue and red spheres correspond to Ag, Si and O atoms respectively. The positive and negative charge density is shown as blue and yellow iso-surfaces respectively at a value of ± 0.07. Two configurations of the, a) typical $[Ag/V_o]^+$ defect, b) $[Ag/V_o]^+$ defect with nearby oxygens.

Each of the 10 sites that did not form a $[Ag/Vo]^+$ complex involved an V_O with a Si-Si bond length less than 2.4 Å, suggesting that the percentage of Ag^+ ions reduced by V_O will be higher than the 72 % found with the sampling method used in this study. Fig. 6 shows the (+1/0) transition energy of the 37 vacancy sites sampled. In 9 of the 37 cases the neutral state was not favoured at any Fermi energy, with the (+1/-1) transitions marked with a star. For each of the complexes, a binding energy was calculated by removing the Ag from the vacancy and placing it in the lowest energy interstital site away from the vacancy. A postive binding energy was found for 10 of the 27 sites with a mean

binding energy of 0.48 eV, each of which may serve as a Ag cluster nucleation site.

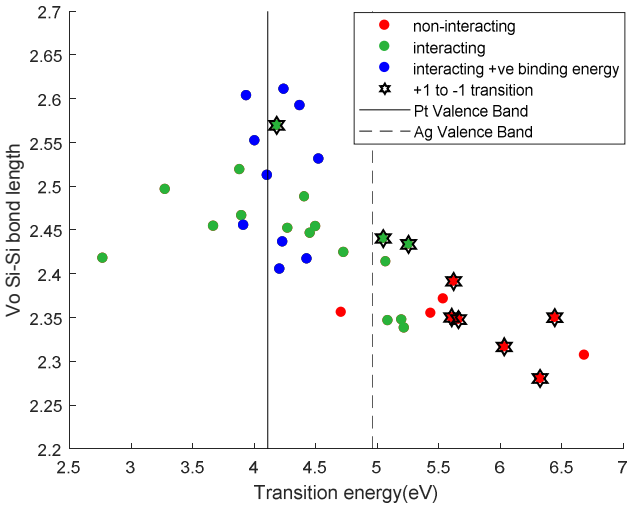

Fig. 6 Scatter diagram showing the +1/0 (dots) and +1/-1 (stars) charge transitions and its correlation to the Si-Si bond length. Red dots represent sites where Ag^+ does not bind to V_O, green dots represent sites where Ag^+ is reduced by V_O and blue dots represent sites where Ag^+ is reduced by V_O and has a positive binding energy.

The neutral charge state of $[Ag/V_O]^0$ is energetically favored at the Fermi energy of Pt for 9 of the 37 sites sampled. This suggests that Ag^+ ions will interact with V_O to form $[Ag/V_O]^+$ complexes, which then trap an electron to form $[Ag/V_O]^0$ near the Pt electrode.

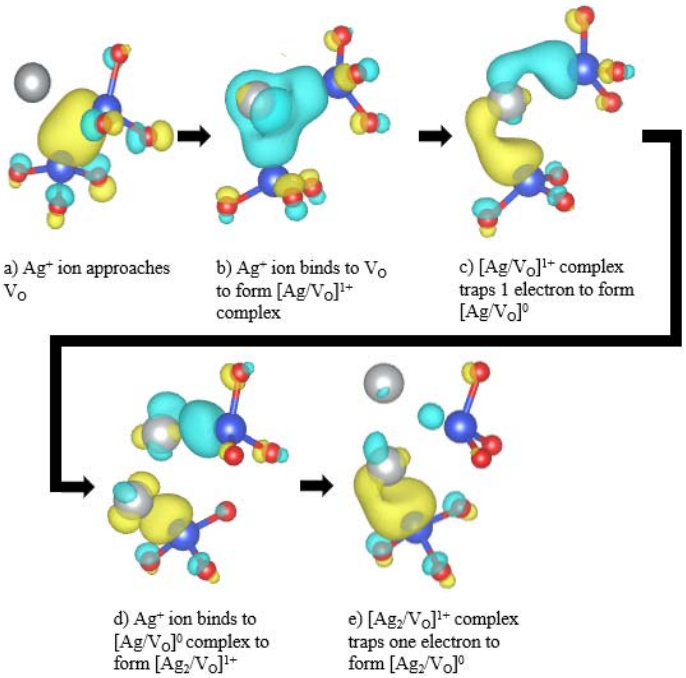

Fig. 7 Schematic showing the V_O as a Ag^+ reduction site and subsequent cluster nucleation site. The silver, blue and red spheres correspond to Ag, Si and O atoms respectively. The positive and negative charge density is shown as blue and yellow iso-surfaces respectively at a value of ± 0.07.

To study the V_O as a cluster nucleation site (Fig. 7), a $[Ag/V_O]$ complex with a (+1/0) transition below the Pt Fermi energy was selected, and a second Ag ion was added to the system. The binding energy of the first Ag^+ to the V_O in this case is 0.6 eV (Fig.7 b). The $[Ag/V_O]^+$ is then favored to trap an electron with the (+1/0) transition at a Fermi energy of 3.9 eV compared to Pt at 4.11 eV (Fig. 7c). Calculations for the additional Ag^+ ion in the $[Ag_2/V_O]^+$ state compared to occupying an interstitial site away from the vacancy give a binding energy of 0.6 eV for Ag^+ to $[Ag/V_O]$ (Fig. 7d). The (+1/0) transition of the $[Ag_2/V_O]$ complex was found to be at 3.6 eV, showing that the $[Ag_2/V_O]^+$ complex would then be favored to trap an electron from the Pt electrode to form $[Ag_2/V_O]^0$ (Fig. 7e). Though a more complete sampling of the Ag_i/V_O interaction is required, it is clear V_O plays a crucial role in clustering.

IV. Conclusion

Two configurations of the Ag^0 interstitial were found. In the first, Ag^0 occupies a void in the lattice, with the HOMO consisting primarily of Ag s-character. The second involves the widening of an O-Si-O bond angle, and a subsequent charge donation from Ag to Si. The Ag^+ interstitial was found to maintain a nearest neighbor distance of 2.2 - 2.6 Å to an O in the lattice. The correlation of incorporation energy to the steric crowing around Ag by the lattice suggests that Ag will traverse a-SiO_2 *via* a void crossing mechanism.

The Ag^+ interstitial defect was found to have the lowest defect formation energy at the Fermi energies of Ag and Pt, though the proximity of the (+1/0) transition to the Ag Fermi energy suggests Ag^0 will be favored under bias. The Ag^+ interstitial is favored at the Pt Fermi energy, suggesting Ag^+ ions are not reduced at the Pt electrodes *via* electron tunneling. Instead, Ag^+ ions are reduced by O vacancies after forming $[Ag/V_O]^+$. $[Ag/V_O]^+$ are then able to trap an electron to form an $[Ag/V_O]^0$. Due to biases introduced in the sampling method, it can be assumed that the rate of Ag^+ reduction is higher than calculated in this study. A second Ag^+ ion can bind to $[Ag/V_O]^0$ to form $[Ag_2/V_O]^+$, which is again favored to trap an electron giving a Ag_2 dimer bound to a V_O $[Ag_2/V_O]^0$, suggesting the V_O site is a strong candidate for Ag cluster nucleation.

Acknowledgements

The A*STAR Graduate Academy is acknowledged for its graduate scholarship under the ARAP program. We also acknowledge funding provided by EPSRC (EP/L015862/1) and the use of the ARCHER High Performance Computing Facility *via* membership to the UK's HPC Materials Chemistry Consortium which is funded by EPSRC (EP/L000202).

References

[1] T.-C. Chang, K.-C. Chang, T.-M. Tsai, T.-J. Chu, and S. M. Sze, "Resistance random access memory," *Mater. Today*, vol. 19, no. 5, pp. 254–264, 2016.

[2] A. Mehonic *et al.*, "Electrically tailored resistance switching in silicon oxide," *Nanotechnology*, vol. 23, no. 45, p. 455201, 2012.

[3] Y. Yang, P. Gao, S. Gaba, T. Chang, X. Pan, and W. Lu, "Observation of conducting filament growth in nanoscale resistive memories," *Nat. Commun.*, vol. 3, p. 732, 2012.

[4] A. C. T. van Duin, A. Strachan, S. Stewman, Q. Zhang, X. Xu, and W. A. Goddard, "ReaxFFSiO Reactive Force Field for Silicon and Silicon Oxide Systems," *J. Phys. Chem. A*, vol. 107, no. 19, pp. 3803–3811,

2003.

[5] S. Plimpton, "Fast Parallel Algorithms for Short-Range Molecular Dynamics," *J. Comput. Phys.*, vol. 117, no. 1, pp. 1–19, 1995.

[6] H. J. C. Berendsen, J. P. M. Postma, W. F. van Gunsteren, A. DiNola, and J. R. Haak, "Molecular dynamics with coupling to an external bath," *J. Chem. Phys.*, vol. 81, no. 8, pp. 3684–3690, 1984.

[7] M. Guidon, J. Hutter, and J. VandeVondele, "Robust Periodic Hartree−Fock Exchange for Large-Scale Simulations Using Gaussian Basis Sets," *J. Chem. Theory Comput.*, vol. 5, no. 11, pp. 3010–3021, 2009.

[8] J. Vandevondele, M. Krack, F. Mohamed, M. Parrinello, T. Chassaing, and J. Hutter, "Quickstep: Fast and accurate density functional calculations using a mixed Gaussian and plane waves approach," *Comput. Phys. Commun.*, vol. 167, no. 2, pp. 103–128, 2005.

[9] J. Sarnthein, A. Pasquarello, and R. Car, "Structural and Electronic Properties of Liquid and Amorphous SiO_2: An Ab Initio Molecular Dynamics Study," *Phys. Rev. Lett.*, vol. 74, no. 23, pp. 4682–4685, Jun. 1995.

[10] S. Susman *et al.*, "Intermediate-range order in permanently densified vitreous SiO_2: A neutron-diffraction and molecular-dynamics study," *Phys. Rev. B*, vol. 43, no. 1, pp. 1194–1197, Jan. 1991.

[11] B. G. LIPPERT, J. HUTTER, and M. PARRINELLO, "A hybrid Gaussian and plane wave density functional scheme," *Mol. Phys.*, vol. 92, no. 3, pp. 477–488, 1997.

[12] J. VandeVondele and J. Hutter, "Gaussian basis sets for accurate calculations on molecular systems in gas and condensed phases," *J. Chem. Phys.*, vol. 127, no. 11, p. 114105, 2007.

[13] S. Goedecker, M. Teter, and J. Hutter, "Separable dual-space Gaussian pseudopotentials," *Phys. Rev. B*, vol. 54, no. 3, pp. 1703–1710, Jul. 1996.

[14] M. Guidon, J. Hutter, and J. VandeVondele, "Auxiliary Density Matrix Methods for Hartree−Fock Exchange Calculations," *J. Chem. Theory Comput.*, vol. 6, no. 8, pp. 2348–2364, 2010.

[15] W. Martienssen and H. Warlimont, *Springer Handbook of Condensed Matter and Materials Data*. 2005.

[16] S. B. Zhang and J. E. Northrup, "Chemical potential dependence of defect formation energies in GaAs: Application to Ga self-diffusion," *Phys. Rev. Lett.*, vol. 67, no. 17, pp. 2339–2342, Oct. 1991.

[17] S. Lany and A. Zunger, "Accurate prediction of defect properties in density functional supercell calculations," *Model. Simul. Mater. Sci. Eng.*, vol. 17, no. 8, p. 84002, 2009.

[18] D. E. Eastman, "Photoelectric Work Functions of Transition, Rare-Earth, and Noble Metals," *Phys. Rev. B*, vol. 2, no. 1, pp. 1–2, Jul. 1970.

[19] N. F. and A. O. and K. M. and S. Miyazaki, "Evaluation of valence band top and electron affinity of SiO 2 and Si-based semiconductors using X-ray photoelectron spectroscopy," *Jpn. J. Appl. Phys.*, vol. 55, no. 8S2, p. 08PC06, 2016.

[20] Y.-C. Yeo, P. Ranade, T.-J. King, and C. Hu, "Effects of high-κ gate dielectric materials on metal and silicon gate workfunctions," *IEEE Electron Device Lett.*, vol. 23, no. 6, pp. 342–344, 2002.

[21] A. M. El-Sayed, M. B. Watkins, A. L. Shluger, and V. V. Afanas'Ev, "Identification of intrinsic electron trapping sites in bulk amorphous silica from ab initio calculations," *Microelectron. Eng.*, vol. 109, pp. 68–71, 2013.

[22] D. Z. Gao, A.-M. El-Sayed, and A. L. Shluger, "A mechanism for Frenkel defect creation in amorphous SiO_2 facilitated by electron injection," *Nanotechnology*, vol. 27, no. 50, p. 505207, 2016.

[23] J. D. Mcbrayer, R. M. Swanson, and T. W. Sigmon, "Diffusion of Metals in Silicon Dioxide," no. June, pp. 1242–1246, 1986.

[24] S. Tappertzhofen, I. Valov, T. Tsuruoka, T. Hasegawa, R. Waser, and M. Aono, "Generic Relevance of Counter Charges for Cation-Based Nanoscale Resistive Switching Memories," *ACS Nano*, vol. 7, no. 7, pp. 6396–6402, Jul. 2013.

[25] Y. Wimmer, A.-M. El-Sayed, W. Gös, T. Grasser, and A. L. Shluger, "Role of hydrogen in volatile behaviour of defects in SiO_2-based electronic devices," *Proc. R. Soc. A Math. Phys. Eng. Sci.*, vol. 472, no. 2190, Jun. 2016.